Proc. of the 11 Int. School on Theoretical Physics Symmetry and Structural Properties of Condensed Matter, Rzeszów 2014

Symmetry-Induced Hybridization in Hexagonal and Zinc-Blende CrTe Crystals

M. Kuzma*

University of Rzeszów, Faculty of Mathematics and Natural Sciences, S. Pigonia 1, 35-959 Rzeszów, Poland

Transition metal chalcogenides of a zinc-blende structure are theoretically predicted to be half metallic and, therefore, they are interesting for spintronic applications. However, the ground state of these compounds is hexagonal, of NiAs type, whereas the cubic phase is a metastable one. Here, we investigate the Cr–Te bondings of both phases of Cr–Te from point of view of symmetry. The hybridization in octahedral and tetrahedral lattice is studied for both structures. The fiber bundle presentation of the hybridization problem is also addressed.

DOI: 10.12693/APhysPolA.128.185

PACS: 61.50.Ah, 75.50.Cc, 75.50.Pp

1. Introduction

Transition metal chalcogenides show metallic or semiconducting properties, depending on the anions and the ratio between the metal and chalcogen atoms. Moreover, these compounds exhibit various types of magnetic properties for different structures and compositions: ferromagnetic, antiferromagnetic or non-collinear spin arrangement. The Cr–Te system is particularly interesting, while — among other Cr chalcogenides — only CrTe shows ferromagnetic properties at room temperature (e.g. CrSe, CrS are antiferromagnets) [1]. It forms several crystal phases $Cr_{1-x}Te$ of a hexagonal NiAs type crystal structure. Much attention has been devoted to half-metallicity of CrTe. However, this property is discovered in Cr–Te zinc-blende (ZB) only, which is not a stable phase of CrTe. In paper [2], the stability of transition-metal pnictides (MnAs, CrAs, CrSb) has been studied by first principles methods. From the calculations, it follows that the energy of ZB phases of pnictides exceeds the energy of the ground state NiAs phases by about 1 eV/f.u. In the case of chalcogenides, this difference of energy is about two or three times smaller [1–3], which makes this compounds preferable for the experimental fabrication of proper (room Curie temperature, adequate thickness of epitaxial layers, stability against distortions, etc.) half-metallic ferromagnets for spintronic applications. Some attempts to stabilize the ZB phase of chalcogenides have been proposed using the following methods: (1) choosing a substrate with a coherent lattice constant for epitaxial growth of the layers [4]; (2) pressure inducing of crystal and magnetic structure of material [5, 6]; doping with magnetic or nonmagnetic ions [7]. However, the stabilization of the ZB phase of chalcogenides is still an open task. We investigate the properties of the chemical bonds in both structures of the NiAs type phases and the zinc-blende one. The results make it possible to design a new method for growth of the ferromagnetic ZB phase of CrTe. Therefore, the aim of this paper is a group-theoretical analysis of the hybrids forming two types of clusters: tetrahedral and octahedral ones, which form the simplest clusters of the cubic and hexagonal phases of CrTe, respectively. Moreover, based on the Racah–Wigner approach and the formalism of the action of a symmetry group on a set [8, 9], we treat the hybrids as a fiber bundle.

2. Crystal structure of cubic and hexagonal CrTe

$Cr_{1-x}Te$ systems crystallize in monoclinic hexagonal NiAs structure [10, 11], with Cr atoms at the sites (0,0,0) and (0,0,1/2), and Te atoms at the sites (1/3,2/3,1/4) and (2/3,1/3,3/4) (Fig. 1a). The elementary cell is presented in Fig. 1a. Cr atoms, as well as Te atoms, form hexagonal layers separately, and they are arranged perpendicularly to the z axes, at the distance $c/2$ (c = 6.222 Å). Each Cr atom is surrounded by six Cr atoms in the xy plane, at the distance a = 3.997 Å. Along the z axes, the distance Cr–Cr is shorter, equal to $c/2$.

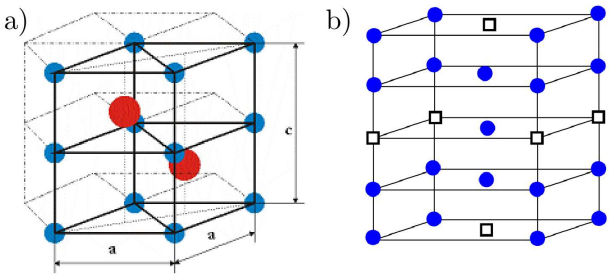

Fig. 1. Crystal structure of NiAs and the elementary cell of CrTe (a), crystal structure of the Cr sublattice of Cr_2Te_3 (b).

The deviation of stoichiometry in the CrTe system, shown by the index x in $Cr_{1-x}Te$, results in various phases with the same symmetry, but a great number of

*e-mail: kuzma@ur.edu.pl

the Cr vacancies. Non-stoichiometric phases may crystallize in the trigonal space group $P3m$. As an example, the arrangement of Cr atoms and its vacancies in the Cr_2Te_3 ($x = 0.33$) crystal lattice is shown in Fig. 1b. The experimentally determined — through the X-ray diffraction (XRD) measurements — crystal data of more popular phases of CrTe have been collected in Table I. The main physical properties of particular phases are indicated in this table as well.

TABLE I

XRD and magnetic data of the $Cr_{1-x}Te$ phases. Crystal parameters are taken from crystal data cards: a — ASTM 00-050-1153, b — ASTM 01-086-2500, c — ASTM 01-086-2506, d — ASTM 65-2312 B, e — ASTM 71-2245, f — ASTM 00-050-1153, g — ASTM 65-6816. Magnetic data are taken from papers of Dijkstra et al. [10, 11].

	CrTe				Cr_3Te_4	Cr_2Te_3	Cr_5Te_8	Cr_5Te_6
composition	0	0–0.13			0.13–0.31		0.33	
crystal structure	cub.	hex. 1	hex. 2	hex. 3	monoc.	hex.	hex. monoc. [1] trig. [1]	hex.
a [Å]	6.29	3.90	6.82	3.99	6.84	6.814	7.815	13.935
b [Å]		3.90	6.82	3.99	3.89	12.073	7.815	3.954
c [Å]		6.00	12.07	6.22	12.53	1.77	11.989	6.857
c/a		1.53	1.76	1.55	1.83		1.53	2.03
α [deg]		90	90	90	91.13		90	
β [deg]		90	90	90			90	
γ [deg]		120	120	120			120	
	[3]	[a]	[b]	[c]	[d]	[e]	[f]	[g]
exchange splitting Cr 3d between ↑↓ [eV]		2.87			2.82	2.74		
magnetic moment [μ_B]				3.51	3.32	3.03		
T_c [K]	327 [12]	340			315–340	117		
$N(E_F)$ [1/eV unit cell]					4.96↑, 1.08↓			

3. Hybrids in cubic lattice of CrTe

The zinc blende structure of a cubic lattice of CrTe consists of tetrahedral clusters in which each Cr atom is surrounded by four Te atoms, and vice versa (Fig. 2). These two kinds of atoms are connected together by hybrid bonds of a σ and π type. In Fig. 2, the σ hybrids are depicted as atom bonds σ_1, σ_2, σ_3, σ_4.

The symmetry of the crystal structure presented in Fig. 2 is T_d (Table II). The same symmetry is revealed in the system of hybrids σ_i, $i = 1, \ldots, 4$. These hybrids form a Γ_σ representation of the group, which is equivalent to the positional representation P of Te atoms marked by the numbers $i = 1, \ldots 4$. Aiming to determine the symmetry of the π hybrids, the local reference system in each position of the Te atom is established, so that the z axis in each node n is directed towards the Cr atom. The characters of the Γ_σ, Γ_π representations have been collected in Table II.

The decomposition of the reducible representations Γ_σ, Γ_π into an irreducible one is as follows:

$$\Gamma_\sigma = A_1 + T_2,$$

$$\Gamma_\pi = E + T_1 + T_2. \quad (1)$$

In the T_d group, the atomic orbitals s, p, d transform according to these representations, as in Table III:

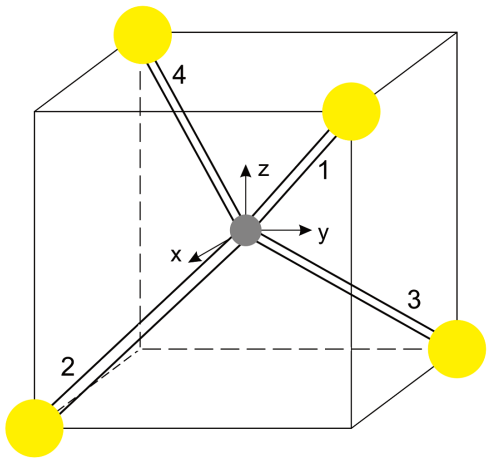

Fig. 2. Tetrahedral structure of the hybrids in zinc-blende CrTe.

s	A_1
p_x, p_y, p_z	T_2
d_{xy}, d_{xz}, d_{yz}	T_2.

Taking into account the electron configuration of Cr and Te atoms (Table IV), the hybrids of the σ type in cubic CrTe are sp^3, or sd^3. The lowest d orbitals

of Cr atoms are $3d$ and the lowest p orbitals of Te are $5p$. Therefore, the hybridization is pd and it shows a T_2 symmetry.

TABLE II

Irreducible representations of T_d group and the Γ_σ and Γ_π hybrid representations.

T_d	E	$8C_3$	$3C_2$	$6S_4$	6σ
A_1	1	1	1	1	1
A_2	1	1	1	-1	-1
E	2	-1	2	0	0
T_1	3	0	-1	1	1
T_2	3	0	-1	-1	1
Γ_σ	4	1	0	0	2
Γ_π	8	0	0	0	2

TABLE III

Transformation of the s, p and d atomic orbitals, according to irreducible representations of the D_{3h}, D_{3d}, T_d and O_h groups.

Orbitals	D_{3h}	D_{3d}	Orbitals	T_d	O_h
s	A_1'	A_{1g}	s	A_1	A_{1g}
p_x	E'	E_u	p_x	T_2	T_{1u}
p_y			p_y		
p_z	A_2''	A_{2u}	p_z		
d_{xz}	E''	E_g	d_{xz}	T_2	T_{2g}
d_{yz}			d_{yz}		
d_{xy}	E'	E_g	d_{xy}		
$d_{x^2-y^2}$			$d_{x^2+y^2}$		
$d_{x^2+y^2}$	A_1'	A_{1g}	$d_{x^2-y^2}$	E	E_g
d_{z^2}	A_1'	A_{1g}	d_{z^2}		

TABLE IV

Electron configuration of Cr, Cd, and Te atoms.

Atom	No. of electrons	Configuration	Excited configuration
Cr	24	$1s^2 \ldots 3d^5 4s$	$4p$
Cr^{2+}	22	$1s^2 \ldots 3d^4$	
Te	52	$1s^2 \ldots 5p^4$	$5d$
Cd	48	$1s^2 \ldots 5d^{10} 5s^2$	$6p$

4. Hybrids in hexagonal lattice of CrTe

The hexagonal structure of CrTe is presented in Fig. 3.

Each Te atom is surrounded by six Cr atoms forming a cluster with a D_{3h} symmetry (Fig. 4a).

Aiming to form hybrids of a σ and π type between Te and Cr atoms, in each node of the Cr atom in Fig. 4a, a local frame system is established, with the z axis directed towards the central atom. The σ and π hybrids form reducible representations of the D_{3h} group. They have been collected in Table Va.

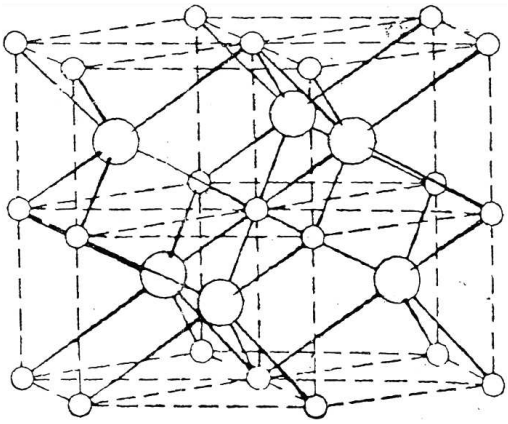

Fig. 3. Hexagonal structure of CrTe (small balls represent Cr atoms, $r_{Cr} = 1.223$ Å, large balls are Te atoms, $r_{Te} = 2.037$ Å).

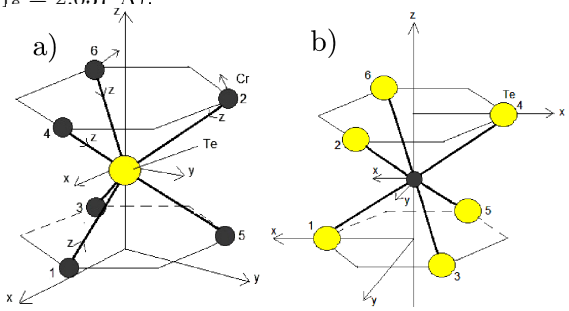

Fig. 4. Symmetry D_{3h} and D_{3d} of the nearest neighbourhood of Te (a) and Cr (b) atoms, respectively, in hexagonal CrTe.

TABLE V

Characters of the D_{3h} (a) and D_{3d} (b) groups and the characters of the Γ_σ and Γ_{π_x}, Γ_{π_y} representations.

(a)

C_{3v}	D_{3h}	E	$2C_3$	$3C_2$	σ_h	$2S_3$	$3\sigma_d$
A_1	A_1'	1	1	1	1	1	1
A_2	A_2'	1	1	-1	1	1	-1
E	E'	2	-1	0	2	-1	0
	A_1''	1	1	1	-1	-1	-1
	A_2''	1	1	-1	-1	-1	1
	E''	2	-1	0	2	1	0
	P	6	0	0	0	0	2
	$\Gamma_{\pi x}$	6	0	0	0	0	-2
	$\Gamma_{\pi y}$	6	0	0	0	0	2

(b)

	D_{3d}	E	$2C_3$	$3C_2$	i	$2S_6$	$3\sigma_d$
	A_{1g}	1	1	1	1	1	1
	A_{2g}	1	1	-1	1	1	-1
	E_g	2	-1	0	2	-1	0
	A_{1u}	1	1	1	-1	-1	-1
	A_{2u}	1	1	-1	-1	-1	1
	E_u	2	-1	0	-2	1	0
	Γ_σ	6	0	0	0	0	2
	$\Gamma_{\pi x}$	6	0	0	0	0	-2
	$\Gamma_{\pi y}$	6	0	0	0	0	2

Decomposition of the hybrid representations into irreducible representations of the D_{3h} group is

$$\Gamma_\sigma = P = A_1' + A_2'' + E' + E'',$$

$$\Gamma_{\pi x} = A_2' + A_1'' + E' + E'',$$

$$\Gamma_{\sigma y} = A_1' + A_2'' + E' + E''. \quad (2)$$

The nearest surrounding of the Cr atoms (Fig. 4b) is different with respect to the neighborhood of Te. The symmetry of the $CrTe_6$ cluster is D_{3d}. In this group, the Γ_σ and Γ_π hybrid representations have been collected in Table Vb. Their decomposition is

$$\Gamma_\sigma = P = A_{1g} + A_{2u} + E_g + E_u,$$

$$\Gamma_{\pi x} = A_{2g} + A_{1g} + E_g + E_u,$$

$$\Gamma_{\sigma y} = A_{1g} + A_{2u} + E_g + E_u. \quad (3)$$

Choosing a new reference system XYZ in Fig. 4b, with Z axis passing through Cr atoms, e.g. No. 2 and No. 5, the cluster $CrTe_6$ forms octahedron and its symmetry is much reacher (O_h — see Fig. 5).

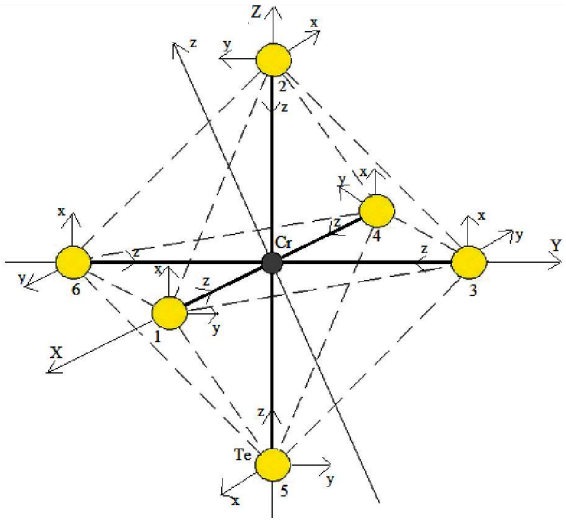

Fig. 5. Octahedral structure of the Te atoms surrounding Cr atoms in CrTe.

In this case, for a proper description of the hybrids, it is convenient to provide — in each node of Te atoms — a local reference system, with the Z axis directed towards the central atoms, as it was done in the previous examples. In such a symmetry group, it is not possible to divide the Γ_π representation into two representations $\Gamma_{\pi x}$ and $\Gamma_{\pi y}$, while the x and y vectors do not form two separate orbits of the O_h group. Hybrid representations are collected in Table VI.

Decomposition of the Γ_σ and Γ_π representations is as follows:

$$\Gamma_\sigma = A_{1g} + E_g + E_{1u},$$

$$\Gamma_\pi = T_{1g} + T_{2g} + T_{1u} + T_{2u}. \quad (4)$$

TABLE VI

Characters of the irreducible representations of the O_h group group and the characters of the Γ_σ and Γ_π representations.

D_h	E	$8C_3$	$6C_2$	$6C_4$	$3C_4^2$	i	$6S_4$	$8S_6$	$3\sigma_h$	$6\sigma_d$
A_g	1	1	1	1	1	1	1	1	1	1
A_{2g}	1	1	−1	−1	1	1	−1	1	1	−1
E_g	2	−1	0	0	2	2	0	−1	2	0
T_{1g}	3	0	−1	1	−1	3	1	0	−1	−1
T_{2g}	3	0	−1	1	−1	3	1	0	−1	−1
A_{1u}	1	1	1	1	1	−1	−1	−1	−1	−1
A_{2u}	1	1	−1	−1	1	−1	1	−1	−1	1
E_u	2	−1	0	0	2	−2	0	1	−2	0
T_{1u}	3	0	−1	1	−1	−3	−1	0	1	1
T_{2u}	3	0	1	−1	−1	−3	1	0	1	−1
Γ_σ	6	0	0	2	2	0	0	0	4	2
Γ_π	12	0	0	0	−4	0	0	0	0	0

5. Fiber structure of hybrids

The positions of atoms in the R cluster are nodes 1,2,3,...,N.

$$R = \{1, ..., N\}. \quad (5)$$

The nodes form a positional space P [8]:

$$P = LC\{e_r \mid r \in R\}, \quad (6)$$

so that P is the space of all the linear combinations of the nodes over the C field of complex numbers.

In each node, there is an atom having atomic orbitals (AO). These form a single-centre AO space. The configurational space L of the system is a tensor product

$$L = P \otimes AO. \quad (7)$$

The configuration space L can be illustrated by a fiber bundle. Let the nodes $r \in R$ be described by a function of the unitary space W_r. The isomorphism $\varphi_r : W \longrightarrow W_r$ maps a certain model space W onto W_r. Let E be a sum

$$E = \cup_{r \in R} W_r.$$

The structure (E, R, W, p) is fiber bundle, with R being the base space, and W being the standard fiber. The fiber bundle scheme of p hybrids in a molecule consisting of 9 atoms is presented in Fig. 6.

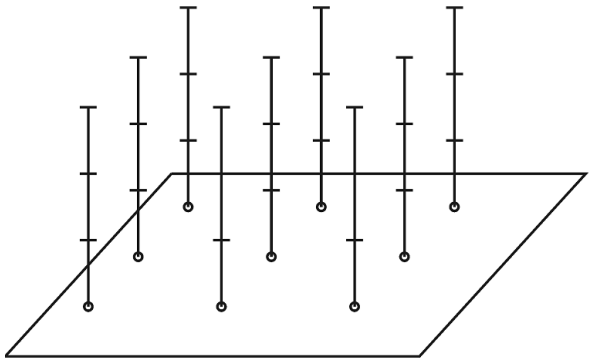

Fig. 6. Fiber bundle model of the hybrids in a molecule consisting of 9 atoms.

The action of the symmetry group G of a cluster in the configurational space L forms the mechanical representation M, which is the product of

$$M = R \otimes V, \tag{8}$$

where R is a transitive representation of the group G, determined by the stability group $H \subset G$ of node 1,

$$R = R^{G:H}. \tag{9}$$

V is the vector representation in an atomic orbital (AO) space. Both representations, i.e. R and V, are reducible and may be decomposed into irreducible representations of the symmetry group G:

$$R = \Sigma_\Lambda m_{R,\Lambda} \Lambda, \tag{10}$$

$$V = \Sigma_\Delta m_{V,\Delta} \Delta, \tag{11}$$

where $m_{R,\Lambda}$ and $m_{V,\Delta}$ are multiplicity factors.

6. Results and discussion

According to Table III, in the O_h and T_d group, the s, p, d orbitals of Cr atom are transformed as

	O_h	T_d
s	A_{1g}	A_1
d_{x2-y2}, d_{z^2}	E_g	E
p_x, p_y, p_z	T_{1u}	T_2
d_{xy}, d_{xz}, d_{yz}	T_{2g}	T_2.

TABLE VII

Symmetry orbitals for the octahedral and tetrahedral clusters of CrTe (sym. — symmetry, hyb. — type of hybrydization, N — normalization factor).

sym.	Cr atomic orbital	Te	N	Te ligand number 1	2	3	4	5	6	hyb.
				O_h						
A_{1g}	s	s	$\frac{1}{\sqrt{2\cdot 3}}$	1	1	1	1	1	1	$s\sigma$
		p_z		1	1	1	1	1	1	$p\sigma$
E_g	d_{z2}	s or p_z	$\frac{1}{2\sqrt{3}}$	-1	2	-1	-1	2	-1	$s\sigma$
	d_{x2-y2}		$\frac{1}{2}$	1		1	1		-1	$p\sigma$
T_{1u}	p_x	p_x	$\frac{1}{\sqrt{2}}$	1			-1			$s\sigma$
	p_y	s or p_y				1			-1	
	p_z	p_z			1			-1		$p\sigma$
T_{2g}	d_{xz}	p_y, p_x	$\frac{1}{2}$	p_y	p_x		p_x	p_y		$pd\pi$
	d_{yz}				p_y	p_x		p_x	p_y	
	d_{xy}			p_x		p_y	p_y		p_x	
				T_d						
A_1	s	s	$\frac{1}{2}$	1	1	1	1			
		p_z		1	1	1	1			
E	d_{z2}	p_x	$\frac{1}{2}$	1	-1	-1	1			
	$d_{x^2-y^2}$	p_y		1	-1	-1	1			
T_2	s or p_2	p_x	$\frac{1}{2}$	1	1	-1	-1			spσ
		p_y		1	-1	1	-1			
		p_z		1	-1	-1	1			
T_2	d_{yz}	$p_x + p_y$	$\frac{1}{4}$	1	-1	1	-1			$pd\pi$
			$\frac{\sqrt{3}}{4}$	-1	1 -1	1				
	d_{xz}	$p_x + p_y$	$\frac{1}{4}$	1	1	-1	-1			
			$\frac{\sqrt{3}}{4}$	1	1	-1	-1			
	d_{xy}	p_x	$-\frac{1}{2}$	1	1	1	1			

The set of atom orbitals of ligands, i.e. six Te atoms in an octahedron (having 6×4 sp orbitals $= 24$), as well as the set of orbitals of four Te atoms in a tetrahedron (4×4 sp orbitals $= 16$), should have the same symmetry properties.

The symmetry orbitals (symmetry basis of the representations) of the type A, E, T_1, T_2 for both clusters have been calculated by the projection method, and are collected in Table VII. They correspond to the hybrids studied. The bases for the T_{1u} representation forming hybrids π have been omitted, while the p_x, p_y orbitals of ligands interact with the p orbitals of the central ion very weakly.

7. Conclusions

We have provided a comparison of the symmetry properties of Cr–Te hybrid bonds in two different structures of CrTe: a hexagonal one, of a NiAs type, and a cubic one, of a zinc-blende type. It has been noticed that in a hexagonal structure, the bonds form an octahedron $CrTe_6$. In a cubic structure, the analogue cluster is a tetrahedron $CrTe_4$. The coincidence as regards the symmetry of the hybrids for both structures has been shown. Moreover, a similarity between the bases of the hybrids for both structures is an unexpected result. From these studies, we conclude that the symmetry of the zinc-blende phases of CrTe is not the main reason for the difficulty in growing zinc-blende CrTe.

References

[1] I. Galanakis, P. Mavropoulos, *Phys. Rev. B* **67**, 104417 (2003).

[2] B. Sanyal, L. Bergqvist, O. Eriksson, *Phys. Rev. B* **68**, 054417 (2003).

[3] W.-H. Xie, Y.-Q. Xu, B.-G. Liu, *Phys. Rev. Lett.* **91**, 037204 (2003).

[4] Y.-J. Zhao, A. Zunger, *Phys. Rev. B* **71**, 132403 (2005).

[5] V. Kanchana, G. Vaitheeswaran, M. Rajagopalan, *J. Magn. Magn. Mater.* **250**, 353 (2002).

[6] T. Eto, M. Ishizuka, S. Endo, T. Kanamata, T. Kikegawa, *J. Alloys Comp.* **315**, 16 (2001).

[7] K. Nakamura, T. Ito, A.J. Freeman, *Phys. Rev. B* **72**, 064449 (2005).

[8] T. Lulek, *Acta Phys. Pol. A* **57**, 407 (1980).

[9] T. Lulek, M. Szopa, *J. Phys. A Math. Gen.* **23**, 677 (1990).

[10] J. Dijkstra, H.H. Weitering, C.F. van Bruggen, C. Haas, R.A. de Groot, *J. Phys. Condens. Matter* **1**, 9141 (1989).

[11] J. Dijkstra, C.F. van Bruggen, C. Haas, R.A. de Groot, *J. Phys. Condens. Matter* **1**, 9163 (1989).

[12] M.G. Sreenivasan, K.L. Teo, M.B.A. Jalil, T. Liew, T.C. Chong, A.Y. Du, *IEEE Trans. Magn.* **42**, 2691 (2006).